QRB DISCOVERY
journals.cambridge.org/qrb

REPORT

What can be learned about the enzyme ATPase from single-molecule studies of its subunit F_1?

Sándor Volkán-Kacso and Rudolph A. Marcus*

Noyes Laboratory of Chemical Physics, 1200 E. California Blvd., Pasadena, CA 91125, USA

Quarterly Reviews of Biophysics (2017), **50**, e14, page 1 of 13 doi:10.1017/S0033583517000129

Abstract. We summarize the different types of single molecule experiments on the F_1 component of F_OF_1-ATP Synthase and what has been learned from them. We also describe results from our recent studies on interpreting the experiments using a chemical-mechanical theory for these biological motors.

1. Introduction

There is now a substantial body of research on single-molecule studies of the component F_1 of F_OF_1-ATP Synthase (Adachi *et al.* 2007, 2012; Noji *et al.* 1997; Sielaff *et al.* 2008; Spetzler *et al.* 2009; Watanabe *et al.* 2010; Yasuda *et al.* 2001) In the physiological operation of the F_OF_1-ATP synthase the proton transfer between two offset ion channels in the F_O causes its c-ring to rotate. This c-ring rotation induces rotation of the central γ shaft, which controls the chemistry in the F_1 $\alpha_3\beta_3$ ring (Boyer, 1993; Braig *et al.* 2000; Junge & Nelson, 2015; Mukherjee & Warshel, 2011, 2015; Senior, 2007; Walker, 2013; Weber, 2010). In treating this modular structure the system has been studied by a 'divide and conquer' method of separately analyzing the function of the F_1 ring with the embedded shaft. The crystal structure of the F_1-ATPase (Braig *et al.* 2000) provides a starting point for these mechanistic studies (Walker, 2003). The kinetic study of the water-soluble F_1-ATPase, although itself artificial, can play a key role in the understanding of the mechanism of the whole ATP synthase.

In the present paper we summarize (Section 4) what we believe has been learned from the single molecule studies, both experimental and theoretical. When coupled with information extracted from ensemble experiments (Boyer, 1993; Braig *et al.* 2000), single-molecule experiments in the F_1-ATPase can uncover the dynamics of the coupling between the γ rotor and the F_1 stator (Senior, 2007; Weber, 2010), e.g., by probing the rotor angle dependence of the individual substeps in the stator. To realize this potential, structurally interpretable information needs to be extracted from single-molecule experiments. One additional item of the present paper is to illustrate the role of an analytical theory that treats the chemo-mechanics, provides a framework for treating and predicting experimental results, and suggests new experiments. The results reveal features linking single-molecule trajectories with past and future and atomistic simulations.

At the outset it should be stated that although much is being learned from the single molecule studies there are some limitations. The F_OF_1-ATP synthase consists of the two units F_O and F_1 but in the single molecule studies it is the F_1 part, which has been studied thus far. Since there is then no proton gradient across the F_O ion channels to drive, via the c-ring and the γ shaft, the opening and closing of β subunits in the F_1, almost all of the single molecule studies have been performed for the reverse reaction, namely the hydrolysis of ATP (Kamerlin *et al.* 2013), catalyzed by the F_1-ATPase. We note in passing that in some bacteria the F_OF_1-ATP synthase works in reverse, it hydrolyzes ATP to generate ion gradient

* Author for correspondence: Rudolph A. Marcus, Noyes Laboratory of Chemical Physics, 1200 E. California Blvd., Pasadena, CA 91125, USA. Tel.: +1-626-395-6566; Fax: +1-626-792-8485; Email: ram@caltech.edu

and *in vitro* the enzyme can operate in both directions depending on the nucleotide and proton concentration (Pedersen & Carafoli, 1987). With the assumption of the reversible nature of the individual steps in the overall process one then learns details of the mechanism of the ATP synthesis in the system. There are nevertheless some single molecule studies described in Section 2 of ATP synthesis directly using controlled rotation (Adachi *et al.* 2007, 2012). In the absence of F_O driven rotation, the F_1 shaft spontaneously rotates in the hydrolysis direction, but in these controlled rotation experiments the rotation and hence the function can be artificially reversed using magnetic tweezers by forcing the γ shaft to rotate in the opposite direction, thus effectively emulating the function of the F_O.

A second note is that most of the single molecule studies are of a quasistatic nature, in that the rotation of the γ subunit is controlled in one way or another. Nevertheless, an important quantity, the timescale of the single-molecule events, is in the millisecond to second range, which is typical for the intact F_OF_1-ATP synthase. This value contrasts with the 'free rotation' microsecond range when the concentration of ATP is high and there is no load on the rotor. Novel information on the F_1-ATPase is being obtained from these experiments on a fine 'scale' not physiologically accessible. In summary, much is being learned about the various dynamic aspects that one can expect to apply in the F_OF_1-ATP synthase.

The single-molecule studies are of various types: stalling, controlled and free rotation, FRET, AFM, and polarized fluorescence. Recently, we have interpreted some of these single-molecule results in terms of a reaction rate theory that combines the chemistry with the mechanical contribution associated with the motor. These studies are complementary to earlier studies largely of ensemble measurements (cf. Boyer, 1993 and references therein). To this end we describe a chemical-mechanical theory (Volkán-Kacsó & Marcus, 2015) that we have formulated to treat several types of single-molecule experiments on this biomolecular motor (Adachi *et al.* 2012; Watanabe *et al.* 2012). The theory draws heavily on a theory of electron and other transfers in solution (Marcus, 1968, 1993; Marcus & Sutin, 1985). We show how the torsional elasticity effects (Sielaff *et al.* 2008) in the motor can be coupled in the theory to various physical and chemical processes, such as nucleotide binding and ATP hydrolysis. We focus in the present review on four types of single-molecule experiments that have been performed on the F_1 component depicted in Fig. 1 of the enzyme, F_1F_O-ATPase. A summary of what we believe has been learned from these single molecule studies is given in Section 4.

The functional form of the chemical reaction rate theory that we employ was originally designed for electron transfer reactions. It has been shown nevertheless that the functional form of the reaction rate, more particularly the free energy of activation in terms of the standard free energy of reaction applies to other types of transfer processes within a range $|\Delta G^0| < \lambda$, using a notation introduced later (Lewis & Hu, 1984; Marcus, 1968; Murdoch, 1983).

In this paper we describe in Section 2 various types of single molecule experiments, in Section 3 the theory and its application to single molecule experiments on the F_1-ATPase of thermophilic bacillus PS3 is described, and in Section 4 what has been learned from these single molecule experiments is summarized. In particular, in Section 4.2 a discussion on the dwell angles and substeps in two kinds of F_1-ATPase, thermophilic bacillus and mammalian, is included.

2. Types of single-molecule experiments

2.1 Stalling experiments

In rotor angle manipulation experiments the angle θ of the rotor was externally controlled by magnetic tweezers, while rotation was optically monitored (Adachi *et al.* 2012). In these experiments magnetic beads were attached to the rotor (Fig. 2*a*) and the rotor aligned itself to the direction of a controlling external magnetic field.

An advanced version of these experiments are the stalling experiments (Watanabe *et al.* 2010). In these experiments the freely rotating shaft was allowed to first reach a dwell angle, then the magnetic tweezers were quickly turned on and the rotor shaft immediately assumed a chosen angle θ. The rotor was stalled at this angle for a predetermined time, then released upon which it either moved back to the original dwell or forward to the next dwell, depending on the state of the underlying process (e.g., for ATP binding either ATP-bound or empty) at the moment of release. We note in passing that earlier experiments (described later) have resolved two dwells, the binding dwell (before an 80° substep, cf. Fig. 1*a*) and the hydrolysis dwell (before a subsequent 40° step).

The observed relative number of forward and back events as a function of stall time was given a simple two-state kinetic interpretation (Watanabe *et al.* 2012), which then permitted the determination of forward (k_f) and backward (k_b) rate constants of ATP binding, or other processes. From their ratio, a local thermodynamic property, an equilibrium constant for the reaction step, was also obtained. The angle dependence of the rate constants was explained in terms of the effect of the elastic response of the rotor structure on the free energy of the F_1-ATPase-nucleotide system (Fig. 2*b*) in the model of elastic transfer of nucleotides or other groups (Volkán-Kacsó & Marcus, 2015). Later, we give some of the experimental and theoretical results and then show what can be extracted from these single-molecule experiments.

https://doi.org/10.1017/S0033583517000129 Published online by Cambridge University Press

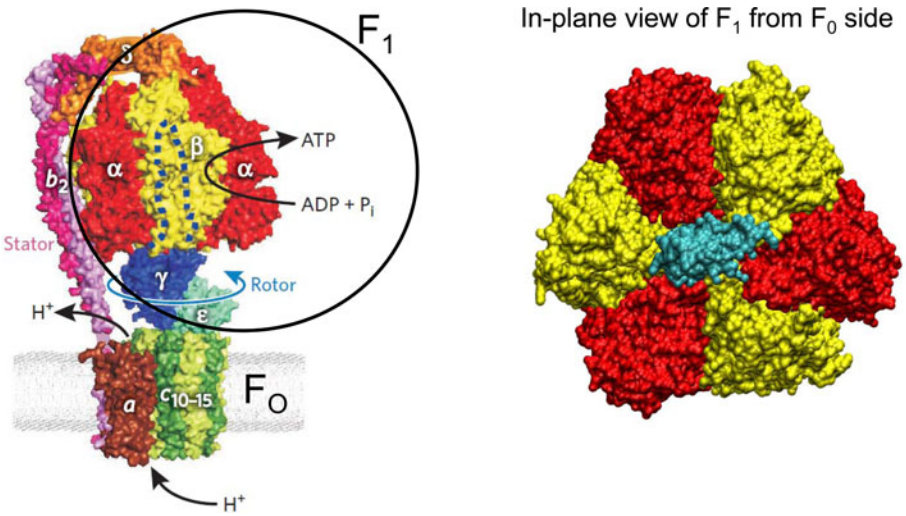

Fig. 1. F-ATPase structure viewed in the plane of the rotor structure (left) and the F_1 subsystem (Braig *et al.* 2000) viewed in the plane of the $\alpha_3\beta_3$ ring (right). The left subfigure was reproduced with journal permission from Weber (Weber, 2010).

2.2 Controlled rotation experiments

In these experiments single-molecule fluorescence microscopy was added to the rotation microscopy and magnetic tweezers (Adachi *et al.* 2012). The individual binding and release events of fluorescent nucleotides were directly monitored, while the shaft was rotated at a constant rate. To detect site occupancy the binding nucleotide species (ATP or ADP) was modified by linking a fluorescent Cy3 moiety to it via a flexible alkane tether (Adachi *et al.* 2007). When the nucleotide was bound to the F_1-ATPase the Cy3 moiety emitted a measurable fluorescence signal but when it was in the solution it was dark. Events whereby the occupancy changed between 0 and 1 were thereby determined and analyzed (Fig. 1*c*). Using a criterion to assign groups of binding events to specific β subunits, in the analysis of Kinosita and co-workers (Adachi *et al.* 2012) the number of $(0 \rightarrow 1)$ and $(1 \rightarrow 0)$ events over the time spent in a 0 and 1 occupancy state yielded forward and reverse rate constants, respectively. Expressions have recently been obtained permitting the extraction of rate constants where multiple events occur, so completing our treatment of single events (Volkán-Kacsó & Marcus, 2017a).

2.3 Free rotation experiments

In the first-generation experiments of this type, the unconstrained rotation of the shaft was observed by conventional microscopy, first under a heavy viscous load via imaging the motion of a microfilament attached to the rotor (Noji *et al.* 1997). Later, the viscous drag was reduced by attaching submicron-sized beads to the rotor (Sakaki *et al.* 2005; Yasuda *et al.* 2001). A counter-clockwise (as defined in the previous section) stepping rotation with dwell angles 120 apart was resolved which later was shown to consist of the 40° and 80° substeps mentioned earlier (Watanabe *et al.* 2010).

2.4 High-speed free rotation experiments

In some later versions of the single-molecule rotation experiments, the size of the imaging bead was further reduced (Yasuda *et al.* 2001). Subsequently gold nanorods (Spetzler *et al.* 2009) were attached to the rotor shaft, now permitting the angular velocity during the transition between steps to be observed. In particular, the gold nanorods do not limit the rotation velocity via their friction with the water molecules. Using a μs resolution imaging of the rotor angle by monitoring the polarization direction of the light scattered by the nanorod, a feature-rich velocity profile was time-resolved, which reflected the intrinsic dynamics of the rotation (Sielaff *et al.* 2016; Spetzler *et al.* 2009).

2.5 Single-molecule FRET and polarization experiments

Another single-molecule fluorescence experiment is a more elaborate version of previous imaging techniques. An example is the single-molecule Förster resonance energy transfer (smFRET) method (Zimmermann *et al.* 2005), which was used in conjunction with rotation imaging to simultaneously monitor subunit conformation changes and rotation (Sugawa *et al.* 2016; Zimmermann *et al.* 2005). Another example is the time-resolved detection of the direction of a bimolecular fluorescence species attached to the β subunit, when the latter undergoes conformational changes (Masaike *et al.* 2008). In the fluorescent probe polarized emission occurs due to a strong dipole moment matrix element coupling the electromagnetic field and the electronic states of the fluorophore along the z axis.

3. Chemo-mechanical group transfer theory

The theory will be described (Volkán-Kacsó & Marcus, 2015, 2016, 2017a) by providing (1) an equation for the

https://doi.org/10.1017/S0033583517000129 Published online by Cambridge University Press

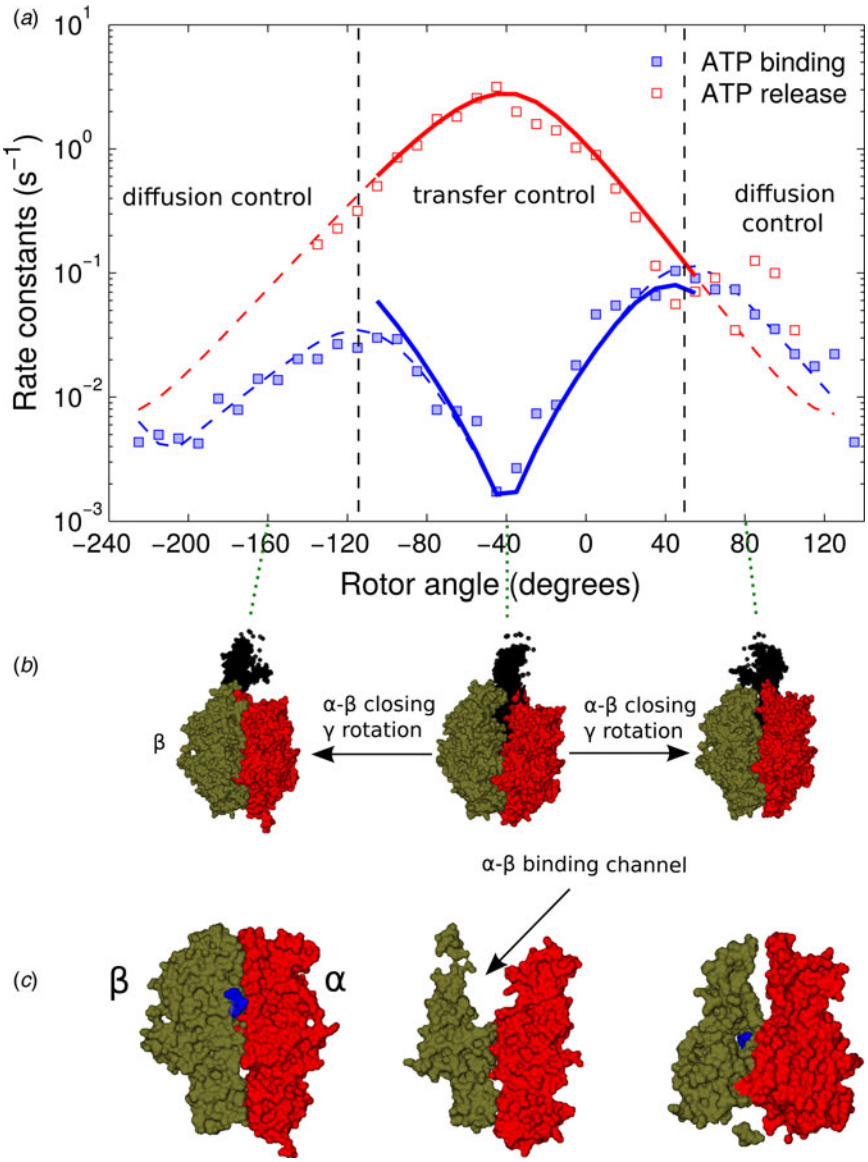

Fig. 2. (*a*) F_1-ATPase in single-molecule imaging and controlled rotation experiments at two rotor angles: 0° and 80°. A double-bead is attached to the γ rotor shaft (in yellow) and rotated against the stator ring (active subunits β_1-β_3). (*b*) Free energy profile for nucleotide binding (k_f) and release (k_b) rate constants at the two angles. (*c*) Open-to-close changes in the nucleotide binding β_1 subunit as a function of rotor angle.

dependence of the rate constant of a substep on the standard free energy reaction, and (2) introducing into the thermodynamic free energy equation a mechanical elastic coupling term arising from the interaction of the subunits with the γ subunit of the F_1-ATPase. The theory and its application to predict controlled rotation data, summarized in this section to make the present review self-contained, is described in more detail in (Volkán-Kacsó & Marcus, 2017b).

3.1 Rate constants and free energy relations

We first note that the equations of the 'weak-overlap' theory of electron transfer reactions were adapted to treat 'strong overlap' reactions, such as the transfer of an atom B in the atom transfer reaction $A + BC \rightarrow AB + C$ (Marcus, 1968) and used for the latter (e.g., Chidsey, 1991; Lewis & Hu, 1984; Murdoch, 1983; Sutin, 1966). In this case the topology is such that there is in effect only one relevant potential energy surface (the lower adiabatic surface) instead of two diabatic surfaces. For such transfer reactions in solution (Marcus, 1968, 1993; Marcus & Sutin, 1985) the free energy barrier for the reaction, $\Delta G^{\ddagger}$, is given by an equation, which has been approximated in the literature by[a]

[a]A relevant equation is a bond energy-bond order equation which has no 'inverted' effect (Marcus, 1968).

https://doi.org/10.1017/S0033583517000129 Published online by Cambridge University Press

$$\begin{array}{ccc} & \Delta G^0(\theta) & \\ G_r^0(\theta) & \rightarrow & G_p^0(\theta) \\ w^r \uparrow & & \downarrow -w^p \\ G_r^0(\theta_i) & \rightarrow & G_p^0(\theta_f) \\ & \Delta G_0^0 & \end{array}$$

Scheme 1. Thermodynamic cycle for a substep showing reactant and product states both when the rotor is stalled at a given angle and when the system is not subject to stalling by the magnetic tweezers.

$$\Delta G^* = \frac{\lambda}{4}(1 + \Delta G^o/\lambda)^2, \tag{1}$$

where, for simplicity of presentation in this paper, we have omitted the 'work terms' that occur in transitioning from a pair of reactants (r) or products (p) in solution to form a collision complex with the F_1-ATPase. In Eq. (1), ΔG^0 denotes the standard free energy reaction of the transfer reaction and λ denotes the 'reorganization energy' for the reaction. The rate constant k is given by

$$k = A \exp(-\Delta G^*/kT) \tag{2}$$

where A depends on the nature of the process, e.g., whether the reaction is first or second order, and on the details of the transition state of the process. A particular example would be to use a collision theory picture (Volkán-Kacsó & Marcus, 2015) of ATP binding to the weak binding site of an empty β subunit in which the pre-exponential term A is a collision frequency Z, and a term related to an ATP binding outside of the β subunit. For the binding and release of ATP there are extensive data obtained by different methods (Adachi *et al.* 2012; Braig *et al.* 2000; Spetzler *et al.* 2009; Watanabe *et al.* 2010, 2012; Yasuda *et al.* 2001). In the ATP binding an ATP first forms a collision complex (Oster & Wang, 2000) with the F_1-ATPase, followed by an ATP binding as the next step (an 80° step) in the overall hydrolysis.

The simplest adaptation of Eq. (1) is to use the quadratic relationship, but, because of the different topology of the surfaces for weak and strong interaction, to set $\Delta G^* = 0$ when $-\Delta G^0 \geqslant \lambda$, and $\Delta G^* = \lambda$ when $\Delta G^0 \geqslant \lambda$ between the reactants. Whereas the ET reaction rate decreases at highly negative ΔG^0 the 'strong overlap' reaction rate reaches some limiting maximum value, a result clear from the topology of the adiabatic surface, instead of experiencing the 'Marcus inverted effect'. When, instead, ΔG^0 is very positive ($\geqslant \lambda$) we use for this limiting case $\Delta G^* = \Delta G^0$. Accordingly, in passing we note that the relation between this model and a bond energy-bond order model (BEBO) has been discussed (Marcus, 1968 and reference cited therein). In the BEBO model the sum of the bond orders in a reaction $AB + C \rightarrow A + BC$ is assumed constant throughout the reaction step, so for an atom or group transfer a cooperative effect is seen. Here, the activation energy when B is transferred from A to C is roughly 10% of the AB bond energy for a thermoneutral reaction. A somewhat more detailed account of the application of the BEBO idea for a substep in the F1-ATPase is found elsewhere (Volkán-Kacsó & Marcus, 2017b). The relevance to processes such as ATP binding is that when an ATP enters a channel in an empty β subunit and finally locks into place in the subunit some hydrogen bonds are broken while new hydrogen bonds are formed, perhaps with an approximately conserving the total number of hydrogen bonds.

3.2 Mechanical elastic coupling

We have used the above ideas (Volkán-Kacsó & Marcus, 2015, 2016, 2017a) in applying Eqs. (1) and (2) to the binding and release of ATP in single-molecule stalling and controlled rotation experiments. The dwell angles 0°, 80°, 120°, 200°, 240°, 320° and 360° are angles of rotation of the rotor with respect to the stator and are the angles of local stability.

A thermodynamic cycle (Scheme 1) was introduced by Volkán-Kacsó & Marcus (2015) to provide a basis for a relationship between the free energies of a ligand binding in free rotation, ΔG_0^0, and the binding free energy $\Delta G^0(\theta)$ at a constant rotor angle θ. We introduced into the expressions for the free energy of the reactants and of the products an elastic coupling (Sielaff *et al.* 2008) between the rotor and the stator (Volkán-Kacsó & Marcus, 2015) involved in the step. In particular, to the two-state model originally used to derive Eq. (1) we added to each parabolic free energy curve an elastic term. The elastic term in the free energy equations for the reactants and products of an individual step in a subunit are given as a function of θ in Eq. (3), so yielding Eqs. (4) and (5) for the free-energy barrier as a function of θ.

$$w^r = \frac{k}{2}(\theta - \theta_i)^2 \quad \text{and} \quad w^p = \frac{k}{2}(\theta - \theta_f)^2, \tag{3}$$

$$\Delta G^*(\theta) = W^r + [\lambda + \Delta G^0(\theta)]^2/4\lambda, \tag{4}$$

where we have now included a work term W^r for attaching the ATP from solution to the exterior of the F_1-ATPase, and where the standard free energy of reaction $\Delta G^0(\theta)$ is given as a function of θ in Eq. (5).

$$\begin{aligned} \Delta G^0(\theta) &= \Delta G_0^0 + w^p(\theta) - w^r(\theta) \\ &= \Delta G_0^0 - k(\theta_f - \theta_i)[\theta - (\theta_f + \theta_i)/2]. \end{aligned} \tag{5}$$

Here, ΔG_0^0 is energy of the final dwell state minus the free energy of the initial dwell state for that step, as in Scheme 1 given earlier.

3.3 Application of theory to the single-molecule experiments

Stalling and controlled rotation experiments provide the θ-dependent rate constants and equilibrium constants for the steps in the overall process. The $\Delta G^0(\theta)$ is related to the θ-dependent equilibrium constant $K(\theta)$ for that step by $\Delta G^0(\theta) = -kT \ln K(\theta)$. The equation for the $\ln K(\theta)$ for the ATP binding step is seen in Eq. (5) to be linear in θ,

https://doi.org/10.1017/S0033583517000129 Published online by Cambridge University Press

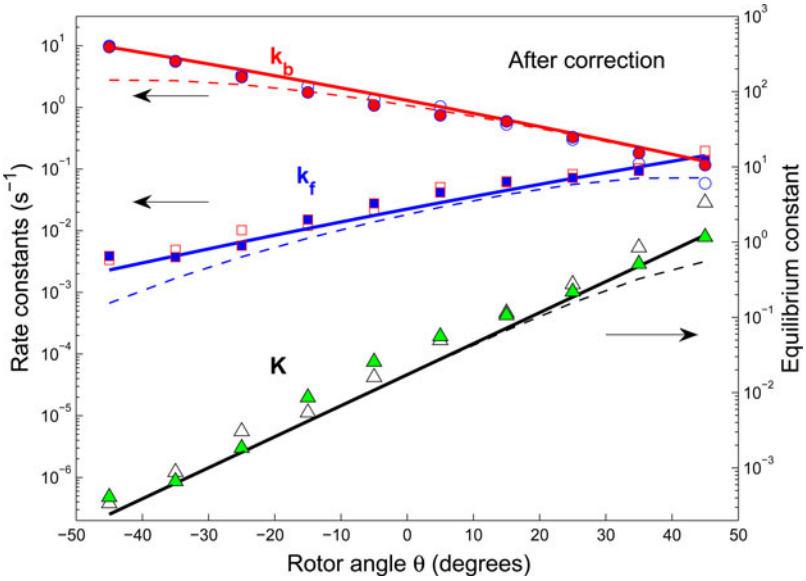

Fig. 3. (Reproduced from Volkán-Kacsó & Marcus, 2016) Corrected binding and release rate and equilibrium rate constants *versus* θ angle for Cy3-ATP in the presence (solid squares, circles and triangles) and absence of Pi (open symbols) in solution. The experimental data (Adachi *et al.* 2012) corrected for missed events (and an error due to replacing the time spent in the empty state by total time of a trajectory) are compared with their theoretical counterparts (solid lines). Dashed lines show the data without corrections.

in agreement with the experimental data in Fig. 1. With experimental data from ensemble (Boyer, 1993; Weber & Senior, 1997) and free rotation (Adachi *et al.* 2012; Spetzler *et al.* 2009; Yasuda *et al.* 2001) experiments Eqs. (4) and (5) were used to predict (Volkán-Kacsó & Marcus, 2015) for the stalling experiments the Bronsted slope $\partial\Delta G^*/\partial\Delta G^0$ of 0·47 which compares with the value of 0·48 in the stalling experiment for the rate of ATP binding and release over the θ range studied. For the binding rate (k_f) the slope of ln k_f (θ) *versus* θ was also predicted for these nucleotides from the Bronsted slope and the ln $K(\theta)$ *versus* θ data, and found to be in reasonable agreement (∼within 10%) with experiment (Volkán-Kacsó & Marcus, 2015). For the spring constant κ of the rotor that appears in Eq. (4) the value of $\kappa = 16$ pN nm rad^{-2} was obtained from the stalling experiments. It was then used in the prediction of the absolute value of the binding and release rate constants in Fig. 3 for the nucleotides in controlled rotation experiments. With no adjustable parameters, good agreement was found between these experiments and our calculations. In the prediction we also used the binding rate constant obtained from the free rotation experiment for the fluorescent ATP species (Spetzler *et al.* 2009). The agreement between experimental and theoretical rate constants is seen in Fig. 3 where the points (symbols) are experimental and the solid curves theoretical.

The controlled rotation experiments are complementary to the other forms of single-molecule experiments in several respects. There is a region of angles θ where the controlled rotation and stalling experiments overlap, so that from the stalling data, supplemented by ensemble data it was possible, as above, to predict results of the controlled rotation experiments using no adjustable parameters. The comparison is given in Fig. 3, covering the θ-range of ∼−40° to ∼+40°. We note that for these rate and equilibrium constant calculations in Volkán-Kacsó & Marcus (2016) we did not use the Bronsted slope equation introduced in the previous study (Volkán-Kacsó & Marcus, 2015), the equation now being simpler than the one involving the Bronsted slope (one equation instead of two). In the controlled rotation experiments there are bound fluorescent nucleotides that become non-fluorescent upon release into the solution and so they are used to observe individual binding and release events, but there will also be some missed events when the rate of release is very fast. It was possible to take into account these missed events using the theory given in the previous equations. The missed events are an example of artifacts that arise in single-molecule trajectories, and theory has been used as an instrument to account for such artifacts (see e.g., Cossio *et al.* 2015 and references therein). The results, after correcting for these events, are given in Fig. 3. The observations of the rates without this correction for the missed events is given by the dashed lines in that figure.

Recently, the theory of elastic group was further extended in several respects (Volkán-Kacsó & Marcus, 2017a). A method was described for predicting the experimentally observed lifetime distribution of long binding events in the controlled rotation. These events involve a combination of two or more processes. Using these distributions the long binding events in the experiments can be treated and the rate constants for the hydrolysis and synthesis reactions occurring during these events extracted. As discussed in a later section a near symmetry of the data about the angle of −40° and a 'turnover' in the binding rate data *versus*

https://doi.org/10.1017/S0033583517000129 Published online by Cambridge University Press

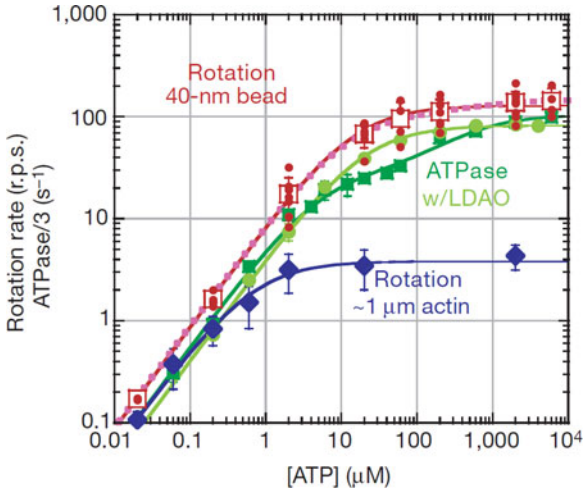

Fig. 4. Comparison of rotation and hydrolysis rates. Red circles, time-averaged rotation rate for individual 40-nm beads. Red squares, rotation rate averaged over different beads. Dark green squares, one-third of the initial rate of ATP hydrolysis. Light green circles, one-third of the rate of ATP hydrolysis in the presence of LDAO. Blue diamonds, rotation rate for an actin filament attached to the g-subunit (reproduced with journal permission from Yasuda *et al.* 2001).

rotor angle for angles greater than ~40° was interpreted using diffusion-reaction kinetics.

4. What has been learned from single-molecule experiments

4.1 The depositing of the F_1-ATPase on the slide does not influence the rotation kinetics

A first question is the relevance of single-molecule studies to the behavior of the actual F_1-ATPase system when in the former the F_1-ATP lies on some surface rather than diffused in solution. In Fig. 4 single-molecule and ensemble kinetic data are plotted as a function of ATP concentration: the rate of the F_1-ATPase rotation in single-molecule experiments and the number of hydrolyzed ATP molecules per 120° rotation in the ensemble experiments.

These Michaelis–Menten curves from single-molecule rotation experiments are practically identical with the corresponding data from ensemble measurements. This important property illustrates that F_1-ATPase molecules attached to a microscope slide and imaged using a filament or a micro bead behave in this respect as if they were simply suspended in solution. Hence, on that basis, the kinetic and dynamic information extracted from single-molecule rotation experiments are relevant to the physiological functionality of the F_1-ATPase.

4.2 There is a concerted kinetics of binding, hydrolysis and release events in the 3 active subunits of the F_1

A scheme shown in Table 1 has been established by a series of single-molecule experiments, in which ATP binding and ADP release (from a different β subunit) are concerted (Beke-Somfai *et al.* 2012) events (80° substep) and ATP hydrolysis and Pi release (again, from a different β subunit) occur during a 40° substep (Watanabe *et al.* 2010).

The single-molecule findings leading to the coupling scheme are the following:

1. *ATP binding occurs during the 80° step*: The dwell before an 80° substep is ATP concentration dependent and the dependence is linear at low concentrations (Michaelis–Menten curve), identifying it as a binding dwell. ATP binding is considered the first step in the kinetic scheme, so the binding dwell is set to 0° (Yasuda *et al.* 2001).
2. *ATP hydrolysis occurs during a 40° step much later in the scheme, namely during the 200° to 240° step*: Mutations at the catalytic pocket have been shown not to affect the 80° step but to reduce the length of the dwell before a 40° step by 2 orders of magnitude, indicating that the hydrolysis occurs during the latter. Using a mixture of ATP and Cy3-ATP, it was shown in fluorescent trajectories that a Cy3-ATP bound at 0° will undergo hydrolysis during the 200° to 240° step (Adachi *et al.* 2007).
3. *ADP release occurs during an 80° step, namely from 240° to 320°*: Using a mixture of ATP and Cy3-ATP, fluorescent Cy3-ATP was seen to undergo hydrolysis (the Cy3-ATP in solution, like ATP, induced the spontaneous rotation in F_1-ATPase) and the resulting fluorescent Cy3-ADP was released during 240° to 320° step (Adachi *et al.* 2007).
4. *Pi release occurs during the last 40° step, from 320° to 360°*: Increasing the concentration of Pi retards the rate of the 40° step, without affecting the 80° step (Adachi *et al.* 2007). In single-molecule experiments this finding is explained by the rebinding of Pi at high Pi concentrations, which will effectively lengthen the dwell before the 40° step. Accordingly, Pi release is associated with a 40° step (Adachi *et al.* 2012), but which of the three? The hydrolysis occurs at 200° to 240°, so Pi release cannot occur before 200°. Stalling experiments showed that the hydrolysis step 200° to 240° is reversible at low Pi concentrations, so Pi remains in the pocket until the last 40° step, namely the 320° to 360° step (Watanabe *et al.* 2010). Accordingly, the release of the P_i is preceded by the ADP release.

A crystallographic method of studying the chemo-mechanics of rotation is to use substitutions in the binding species and thus prepare various stable states that can be resolved in X-ray structure (Bason *et al.* 2014). Using this approach in the case of mammalian (human and bovine) F_1-ATPase Walker and coworkers (Bason *et al.* 2014) found three such states about 65°, 25° and 30° apart. A somewhat similar 80°, 10° and 30° division of the 120° for the dwells of the thermophilic Bacillus ATPase studied in current single-molecule experiments has been suggested (Adachi *et al.* 2007) based on a mutant that retards the rate and permits an improved

https://doi.org/10.1017/S0033583517000129 Published online by Cambridge University Press

Table 1. *Scheme of coupled processes in F_1-ATPase during free rotation*

Angle *versus* subunit	0°	80°	120°	200°	240°	320°	360°
β_1	ATP binding	(ATP)	(ATP)	ATP hydrolysis	ADP release	Pi release	ATP binding
β_2	ADP release	Pi release	ATP binding	(ATP)	(ATP)	ATP hydrolysis	ADP release
β_3	(ATP)	ATP hydrolysis	ADP release	Pi release	ATP binding	(ATP)	(ATP)

The dwell angle increases in the counter clockwise direction. The species occupying the pockets of ring β subunits 1, 2, and 3 are represented in the binding and catalytic dwells.

time-resolution. Kinosita and coworkers (Adachi *et al.* 2007) suggested that the combined 10° and 30° substeps give rise to the 40° substep resolved in previous single-molecule experiments (Nishizaka *et al.* 2004) and associated with hydrolysis and Pi release in a different subunit (Watanabe & Noji, 2014; Watanabe *et al.* 2010). The 10° is presumably the hydrolysis step, a similar small 15° hydrolysis step is supported by a very approximate independent analysis (Volkán-Kacsó & Marcus, 2017b), but the latter can be improved when more accurate kinetic data in the stalling experiments become available. If the highly time-resolved experiments, resolved on the microsecond scale (Sielaff *et al.* 2016), become available at lower ATP concentrations they too can provide relevant data on these divisions of the 120°. So, a further study of the dwell angles is of interest in relating results from these different approaches.

4.3 Unidirectional concerted stepping rotation occurs in the presence of fluorescent ATP and in mutant F1-ATPase species

The kinetics in the F_1-ATPase, when only the fluorescent Cy3-ATP was in the buffer, (there was no ATP), was shown by Kinosita and co-workers (Nishizaka *et al.* 2004) to be practically identical with the kinetics when the rotation was driven by unlabeled ATP. While the chemo-mechanical coupling and the stepping were identical, the average rate of rotation was lower with Cy3-ATP than with ATP, owing to the lower rate of Cy3-ATP binding.

In single-molecule experiments, such as stalling, one of three β subunits was mutated to reduce the hydrolysis and catalysis rates, which was needed to properly resolve and study the catalytic step (Adachi *et al.* 2012). The rates were further reduced by using a slowly hydrolyzing mutant nucleotide analog ATPγS instead of the ATP itself. Again, the stepping, directional rotation and so the coupling scheme was not altered by these changes, only smaller rate constants were seen in the free rotation trajectories (Nishizaka *et al.* 2004).

4.4 Comparison of single occupancy experiments with multiple occupancy experiments and comparison of corresponding rates

The θ-dependent rate of ATP binding is not influenced by the occupancy of the neighboring sites and thus by the total occupancy (Sakaki *et al.* 2005). In the stalling experiments (Watanabe *et al.* 2012) used to study ATP binding, when the rotor angle was stalled at angles ranging from about −45° to +45°, the events of ATP binding and release as a function of stalling time followed a two-state kinetics. During longer stall times multiple binding and release events occurred. When an ATP is first bound, the binding induces a fast release of ADP from the counter clockwise neighbor β subunit (Adachi *et al.* 2007). Given the low ADP concentration maintained in the experiments (to prevent the so-called 'ADP inhibited' state from forming) any subsequent ATP binding and release events occurred with only a Pi in the latter β subunit. Accordingly, whereas the first ATP binding event occurred in the presence of ADP in the second subunit, any ATP release and subsequent ATP binding events occurred without the ADP in the second subunit. Yet, when the stall times for this ATP binding/release step were increased, the statistics of forward and backward steps and hence the θ-dependent rate constant of ATP binding were not altered.

In fluorescent Cy3-ATP free rotation (Adachi *et al.* 2012) and controlled rotation experiments (Watanabe *et al.* 2012) there was no difference in the rate constant of Cy3-ATP binding, even though the site occupancy was 2–3 in the former and only 0 and 1 in the latter. In other experimental studies that accessed very low nM ATP concentration regimes it was also concluded that the rate constant of binding of ATP was not influenced by the nucleotide occupancy in the neighboring subunits (Sakaki *et al.* 2005).

In contrast, the release rate of ADP is determined by whether ATP is bound or not to a neighboring site. In the chemo-mechanical scheme given in Table 1 the ADP release during the 80° step is faster than 1 s^{-1}. This upper limit is due to the rate limiting hydrolysis step seen in the high-resolution single-molecule rotation experiments (Yasuda *et al.* 2001). Meanwhile, the spontaneous release rate of ADP, i.e., when it is not induced by the binding of an ATP to the clockwise neighbor, is, very slow, on the order of tens of seconds (Adachi *et al.* 2012). Consequently, the binding of ATP accelerates the release of ADP in the counter clockwise subunit by at least 4 orders of magnitude, reflecting the role of conformational changes induced by the binding.

https://doi.org/10.1017/S0033583517000129 Published online by Cambridge University Press

The above observations have been used in our theoretical treatment of ATP binding and release rates in controlled rotation and stalling experiments (Volkán-Kacsó & Marcus, 2015, 2016, 2017a). They establish the condition that the 80° step is controlled by the ATP binding/release events in a single β subunit: these events induce opening and closing conformational changes in that subunit while any changes in the other two subunits would 'tag along'. Using a single reaction coordinate associated with the first β subunit, the changes in the latter were taken into account (Volkán-Kacsó & Marcus, 2015).

4.5 The concerted kinetics in the ring subunits drives a unidirectional rotation kinetics even in the absence of a rotor shaft

High-speed AFM measurements (Uchihashi *et al.* 2011) in a rotorless F_1-ATPase demonstrated that the opening-closing kinetics of the β subunits follow a unidirectional counter-clockwise rotation pattern. The result is consistent with the kinetic scheme in the counter-clockwise rotation observed in the complete F_1, albeit the individual steps in the rotorless F_1-ATPase are slower. Using the rotation pattern, Noji and coworkers (Uchihashi *et al.* 2011) extracted the rotation rate constant *versus* ATP concentration reproduced in Fig. 5.

The strong dependence of binding and release rate constants on the rotor angle could suggest, as previously proposed, a so-called 'γ-dictator' model (Uchihashi *et al.* 2011), whereby this concerted mechanism in the hydrolysis and presumably in the synthesis cycles is due to the interaction between rotor and ring subunits, alone. Indeed, our present treatment of controlled rotation experiments indicates that the single-site activity can be described by such a model.

However, when considering higher nucleotide concentrations, in particular in rotation experiments for F_1-ATPase under physiologically relevant conditions, giving rise to a multi-site activity, events of binding/release and hydrolysis/synthesis occurring in pockets of different β subunits are directly coupled. These inter–subunit interactions are strong enough to determine the directional rotation kinetics even without the γ shaft (Uchihashi *et al.* 2011), or a truncated shaft (Furuike *et al.* 2008). So while the angular position θ of the latter does affect the rates of the processes in the β subunits, it is not essential in mediating the interactions between the β subunits that lead to the concerted kinetics.

4.6 Direct information on the opening and closing of the subunits

Several single-molecule experiments have provided methods to monitor the opening-closing kinetics.

1. Optical imaging of F_1-ATPase rotation was used in tandem with single-molecule imaging of polarized light emission from fluorophores attached to a β subunit (Masaike *et al.* 2008). With this arrangement the directional changes of the subunits in the plane of the F_1 ring were monitored. It was demonstrated that in addition to hinge bending conformational changes, these subunits also undergo a twisting motion during the chemo-mechanical cycle.
2. In combined rotation and FRET imaging experiments the subunit conformational changes were monitored while the F_1 underwent typical stepping rotation (Sugawa *et al.* 2016). The FRET signal was analyzed using statistical theoretical methods and showed that in the active F1-ATPase the empty subunit is in an open conformation while the nucleotide-bound subunits are in closed conformations.
3. As described earlier, high-speed AFM measurements were used to monitor the rotary kinetics of opening and closing of the β subunits (Uchihashi *et al.* 2011). As in item 2 above, in these experiments the empty subunits awaiting the binding of an ATP were in an open state, while the other two subunits, presumably with nucleotides in their catalytic pockets, were in a closed state.

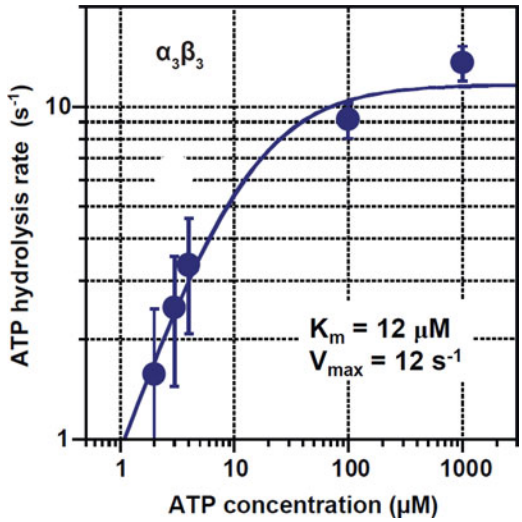

Fig. 5. ATP hydrolysis rate of rotorless F1-ATPase ($\alpha_3\beta_3$ ring only) as a function of ATP concentration. The ATP hydrolysis rate constant extracted from the kinetics inferred from high-speed AFM measurement obeyed Michaelis–Menten kinetics (solid line), reproduced from Noji and co-workers (reproduced with journal permission from Uchihashi *et al.* 2011).

4.7 Exponential rate and equilibrium constant versus rotor angle dependence of binding/release and catalysis

As described in Section 3 stalling and controlled rotation experiments revealed exponential-like forward and back rate constants for ATP binding in the region of angular overlap in these experiments (Adachi *et al.* 2012; Watanabe *et al.* 2012). Such exponential functions apply to the

https://doi.org/10.1017/S0033583517000129 Published online by Cambridge University Press

hydrolysis, Pi release, and various nucleotide binding rates in regions where these events occur in spontaneous rotation. The forward and back rate constants have opposite angle-dependent trends, and the equilibrium constant is strictly exponential, as predicted by theory (Volkán-Kacsó & Marcus, 2016).

4.8 There is a turnover in the ATP binding rate around 80°

The turnover in the ATP binding rate constants *versus* rotor angle plot seen in Fig. 6*a* indicates that the closing of the binding channel continues as the angle is rotated beyond 80°. The turnover is consistent with structural data and the idea of a continuum of open-to-close states between −40° and 140°.

We suggested (Volkán-Kacsó & Marcus, 2016) that a diffusion process while the ATP is entering the channel in the subunit after the initial binding of the ATP to the outside of the F_1-ATPase. The latter then serves as the reactant state in the transfer process. The binding channel leading to the binding pocket (Fig. 6*c*), which closes as the rotor is moved in the positive direction (Fig. 6*b*) retards the diffusion process to the extent that it becomes the bottleneck during binding for angles beyond 50° or so. Conversely, in this standard diffusion-reaction scheme (Marcus, 1960; Noyes, 1961), the transfer reaction is the bottleneck in the θ-region from about −45° to +45° where stalling and controlled rotation experiment overlap.

4.9 Near symmetry of the kinetic data about −40° and about +140°

As seen in Fig. 6*c* the β subunit is the most open at −40° and the most closed presumably at +140° (0° is defined as the binding dwell angle at which the β subunit in question is empty and is about to undergo ATP binding associated with a subsequent 80° substep). The minimum at −40° does not correspond to a specific dwell angle. The structural changes of opening and closing are consistent with the trends of binding/release *versus* rotor angle data and with spontaneous free rotation experiments. In particular:

1. Moving the rotor to the left or right starting from −40° in both cases induces a closing of the β subunit which accelerates binding. This behavior is consistent with the spontaneous forward rotation induced by binding of ATP in free rotation experiments occurring in a θ-range to the right of −40° (from 0° to 80°).
2. Rotating the γ rotor towards −40° from the left or right in both cases induces an opening of the β subunit, which accelerates release. This result, in turn, is consistent with the spontaneous forward rotation induced by the release of ADP in free rotation experiments occurring in a θ-range to the left of −40° (from of −120° to −40°).

A degree of asymmetry is also seen in the binding/release rate *versus* rotor angle data relative to the angle from −40° in both directions: Notably, in the presence of Pi in the solution, ATP binding to the right in Fig. 6*a* occurs at much higher rates than ATP binding to the left. Thus, Pi binding hinders ATP binding in the synthesis direction, but does not prevent ADP binding, a behavior that is consistent with the hydrolysis scheme being the inverse of the synthesis scheme established by single-molecule experiments (Watanabe *et al.* 2010; Yasuda *et al.* 2001). (In the hydrolysis direction Pi is the last to be released during the final 320°–360° substep.)

4.10 In the active F_1-ATPase the Pi release occurs after ADP release

In the chemo-mechanical scheme from Table 1 established by the single-molecule experiments, Pi is the last to be released during the final 320°–360° substep. A corresponding structure, i.e., with ATP in one subunit, ATP (or ADP and Pi) in another subunit and Pi only in the third subunit has yet to be found. This observation raises the possibility that the 'ground state' structure reported in X-ray crystallography (Braig *et al.* 2000) is a stable structure that is not on the kinetic pathway of F_1-ATPase rotation. Based on recent stalling experiments it was suggested that the crystallography structure, in which one subunit appears to contain ADP without Pi, is the so-called ADP inhibited state (Watanabe & Noji, 2014). This result is a reminder that an X-ray structure may sometimes represent the most stable structure and not always the kinetically active structure. It is clear that the structural information is an essential component for understanding the mechanism and that the kinetic data can provide useful additional data for determining the detailed mechanism.

4.11 Angle-dependent rate constants can be extracted from the controlled systems such as stalling or controlled rotation experiments

As seen in Fig. 2, the rate constant *versus* rotor angle are quasi-exponential and in the range of overlap between the two experiments the forward rate constants and the backward rate constant have opposite slopes. The elastic group transfer theory was used to interpret and predict these angle-dependent kinetic (Volkán-Kacsó & Marcus, 2016). Furthermore, we recently devised a method to use the lifetime distribution function of long binding events from the controlled rotation experiments to extract the rate constants for hydrolysis and synthesis (Volkán-Kacsó & Marcus, 2017a). We note that due to the angle dependence of the binding, chemical reaction and release rate constants, these waiting time distributions do not necessarily follow simple exponential dependence, and careful treatment is needed to use the data for extraction of the kinetic properties from these distributions.

https://doi.org/10.1017/S0033583517000129 Published online by Cambridge University Press

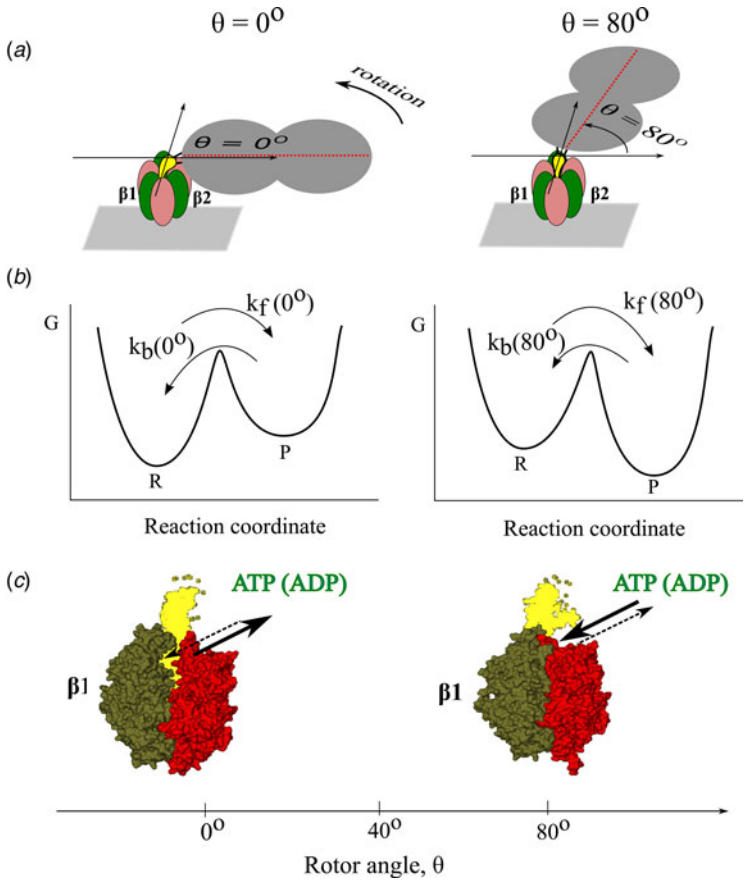

Fig. 6. (*a*) Reported binding and release rate constants *versus* controlled rotation angle for fluorescent ATP in the presence of Pi in solution. The reported uncorrected experimental data (squares) are compared with theoretical counterparts (solid lines) by calculating missed events and also correcting for an error due to replacing the time in the empty state T_0 by the total time T. Dashed lines show a fit to the experimental data. (*b*) F_1-ATPase structure at three different rotor angles with β subunits in green, α subunits in red and the γ subunit in black. (*c*) Cutaway of the three structures revealing the binding channel at the α–β interface and its narrowing as the rotor angle is changed. The figure was reproduced from (Volkán-Kacsó & Marcus, 2017b).

4.12 There is a relation between the rate constants in stalling, controlled and free rotation experiments

The angle-dependent rate constants in Figs 3 and 6 have been used (Volkán-Kacsó & Marcus, 2017b) to calculate the rate constants that can be extracted from the distribution of dwell times in free rotation trajectories. To do so, the fluctuations of the rotor angle about the initial dwell angle were used to calculate the average rate constants (Volkán-Kacsó & Marcus, 2017b). In particular, for the ATP binding step, the initial angle fluctuates about $\theta_i = 0°$ for the forward process or it fluctuates about $\theta_i = 80°$ for the reverse process. The idea of using angle-dependent rate constants, $k_f(\theta)$ and $k_b(\theta)$, arises from an approximation, which is valid on the *ms* to *s* timescales resolved in free rotation experiments. In the latter are used microbeads, in which the stepping in the rotation appears as a discrete process of jumping between subsequent dwells, 0°, 80°, 120°, … In this case, transition state theory and hence a rate description is applicable. A quasi-static θ applies whenever a microbead is used with a slow response time due in part to the friction with the water molecules in the buffer solution.

The rotation rates reported for ATP synthesis in bacterial, mitochondrial and chloroplast enzymes under physiological conditions are slow, about 100 s^{-1} (Cross *et al.* 1982; Etzold *et al.* 1997; Junesch & Gräber, 1985), and are similar to single-molecule studies on F_1-ATPase. The latter probes *ms* to *s* timescales, relevant to the physiologically relevant function. The viscosity-loaded conditions imposed by the use of the microbeads, are also physiologically relevant, as demonstrated by Junge and coworkers (Panke *et al.* 2001), who argued that a compliant rotor running under high load (and hence elastically twisted) is necessary for an efficient coupling between the F_O and F_1, given that their subunit counts are incommensurate.

4.13 There is a harmonic behavior of the restoring force

The Gaussian distribution of the fluctuations about the dwell angle seen in single-molecule experiments (Adachi *et al.* 2012; Sielaff *et al.* 2008) correspond to a harmonic behavior. The elastic behavior is due to the twisting and bending of structural elements in the ATPase, such as the rotor and the β lever arm, described by a spring constant κ (Volkán-Kacsó

https://doi.org/10.1017/S0033583517000129 Published online by Cambridge University Press

& Marcus, 2015). The linearity of the plot of the logarithm of the equilibrium constant *versus* θ supports the assumption that the same κ can be used in the two terms in Eq. (3).

4.14 Using the rate constant versus rotor angle data one can predict the dwell angles and the step size in the free rotation

The theory has provided simple mathematical relations between the dwell angles, the spring constant and log *k versus* θ slopes (Volkán-Kacsó & Marcus, 2016, 2017a) When the logarithm of the ratio of the forward and reverse rate constants is linear in θ the difference of dwell angles bracketing the step can be predicted (Volkán-Kacsó & Marcus, 2017b). To do so an independent estimate of the spring constant is necessary, e.g., from fluctuation experiments (Sielaff *et al.* 2008). Then using the angle-dependent rate constant data from stalling experiments, the difference of dwell angles bracketing the hydrolysis step were predicted from the free rotation trajectories (Volkán-Kacsó & Marcus, 2017b). We note that structurally the hydrolysis step is coupled to structural changes of the ring subunits and thus the γ shaft (Beke-Somfai *et al.* 2013). The linearity condition was not fulfilled for the ATP binding step but was roughly fulfilled for the hydrolysis although the present data are relatively sparse (Fig. 3*c* in Watanabe *et al.* 2012).

4.15 What is not known from current single-molecule experiments

a. The single molecule studies have been performed in the F_1-ATPase and not on the F_OF_1 ATP synthase;
b. Detailed correlation at the atomic level of the shaft rotation in relation to the opening and closing and other conformational changes of the β subunits are not clarified;
c. Improved resolution of the dwell angles.

5. Concluding summary

In summary, single-molecule experiments have revealed a number of new features on the mechanism of F1-ATPase, also relevant for the understanding of the behavior of the complete ATP synthase. Among these features are the following:

a. Similar behavior is found for F1-ATPase on a microscope slide and F1-ATPase dispersed in solution;
b. Concerted kinetics of binding, hydrolysis and release events in the 3 subunits during a rotation with 40° and 80° substeps;
c. In F_1-ATPase rotation hydrolysis occurs 200° after ATP binding and Pi release follows ADP release;
d. The ring subunits drive a unidirectional counterclockwise rotation even in the absence of a rotor shaft;
e. Opening and closing of the β subunits during nucleotide binding and release drive shaft rotation;
f. There are quantitative relations between the rate constants in stalling, controlled and free rotation experiments;

Acknowledgements

It is a pleasure to acknowledge the support of this research by the Office of Naval Research, the Army Research Office, and the James W. Glanville Foundation.

References

Adachi, K., Oiwa, K., Nishizaka, T., Furuike, S., Noji, H., Itoh, H., Yoshida, M. & Kinosita, Jr., K. (2007). Coupling of rotation and catalysis in F1-ATPase revealed by single-molecule imaging and manipulation. *Cell* **130**, 309–321.

Adachi, K., Oiwa, K., Yoshida, M., Nishizaka, T. & Kinosita, Jr., K. (2012). Controlled rotation of the F1-ATPase reveals differential and continuous binding changes for ATP synthesis. *Nat. Comm.* **3**, 1022.

Bason, J. V., Montgomery, M. G., Leslie, A. G. W. & Walker, J. E. (2014). How release of phosphate from mammalian F1-ATPase generates a rotary substep. *Proceedings of the National Academy of Sciences USA* **112**, 6009–6014.

Beke-Somfai, T., Feng, B. & Nordén, B. (2012). Energy phase shift as mechanism for catalysis. *Chemical Physics Letters* **535**, 169–172.

Beke-Somfai, T., Lincoln, P. & Nordén, B. (2013). Rate of hydrolysis in ATP synthase is fine-tuned by a-subunit motif controlling active site conformation. *Proceedings of the National Academy of Sciences USA* **110**, 2117–2122.

Boyer, P. D. (1993). The binding change mechanism for ATP synthase – some probabilities and possibilities. *Biochimica et Biophysica Acta* **1140**, 215–250.

Braig, K., Menz, R. I., Montgomery, M. G., Leslie, A. G. & Walker, J. E. (2000). Structure of bovine mitochondrial F1-ATPase inhibited by Mg2+ADP and aluminium fluoride. *Structure* **8**, 567–573.

Chidsey, C. E. D. (1991). Free energy and temperature dependence of electron transfer at the metal-electrolyte interface. *Science* **251**, 919–922.

Cossio, P., Hummer, G. & Szabo, A. (2015). On artifacts in single-molecule force spectroscopy. *Proceedings of the National Academy of Sciences USA* **112**, 14248–14253.

Cross, R. L., Grubmeyer, C. & Penefsky, H. S. (1982). Mechanism of ATP hydrolysis by beef heart mitochondrial ATPase. Rate enhancements resulting from cooperative interactions between multiple catalytic sites. *Journal of Biological Chemistry* **257**, 12101–12105.

Etzold, C., Deckers-Hebestreit, G. & Altendorf, K. (1997). Turnover number of *Escherichia coli* F_OF_1-ATP synthase for ATP synthesis in membrane vesicles. *European Journal of Biochemistry* **243**, 336–343.

Furuike, S., Hossaih, M. D., Maki, Y., Adachi, K., Suzuki, T., Kohori, A., Itoh, H., Yoshida, M. & Kinosita, Jr., K. (2008). Axle-less F1-ATPase rotates in the correct direction. *Science* **319**, 955–958.

Junesch, U. & Gräber, P. (1985). The rate of ATP synthesis as a function of delta pH in normal and dithiothreitol-modified chloroplasts. *Biochim. Biophys. Acta.* **809**, 429–434.

Junge, W. & Nelson, N. (2015). ATP synthase. *Annual Review of Biochemistry* **84**, 631–657.

Kamerlin, S. C. L., Sharma, P. K., Prasad, R. B. & Warshel, A. (2013). Why nature really chose phosphate. *Quarterly Reviews of Biophysics* **45**, 1–32.

https://doi.org/10.1017/S0033583517000129 Published online by Cambridge University Press

Lewis, E. S. & Hu, D. D. (1984). Methyl transfers. 8. The Marcus equation and transfers between aerosulfonates. *Journal of the American Chemical Society* **106**, 3292–3296.

Marcus, R. A. (1960). Discussion comment on mixed reaction-diffusion controlled rates. *Discuss. Farad. Soc.* **29**, 129.

Marcus, R. A. (1968). Theoretical relations among rate constants, barriers, and Brønsted slopes of chemical reactions. *The Journal of Physical Chemistry* **72**, 891–899.

Marcus, R. A. (1993). Electron transfer reactions in chemistry: theory and experiment. In *Les Prix Nobel* (ed. T. Frangsmyr), p. 63. Stockholm, Sweden: Nobel Foundation Almqvist & Wiksell.

Marcus, R. A. & Sutin, N. (1985). Electron transfers in chemistry and biology. *Biochim. Biophys. Acta.* **811**, 265–322 (and references cited therein).

Masaike, T., Koyama-Horibe, F., Oiwa, K., Yoshida, M. & Nishizaka, T. (2008). Cooperative three-step motions in catalytic subunits of F1-ATPase correlate with 80 degrees and 40 degrees substep rotations. *Nature Structural & Molecular Biology* **15**, 1326–1333.

Mukherjee, S. & Warshel, A. (2011). Electrostatic origin of the mechanochemical rotary mechanism and the catalytic dwell of F1-ATPase. *Proceedings of the National Academy of Sciences USA* **108**, 20550–20555.

Mukherjee, S. & Warshel, A. (2015). Dissecting the role of the γ-subunit in the rotarychemical coupling and torque generation of F1-ATPase. *Proceedings of the National Academy of Sciences USA* **112**, 2746–2751.

Murdoch, J. R. (1983). A simple relationship between empirical theories for predicting barrier heights of electron-transfer, proton-transfer, atom-transfer, and group transfer reactions. *Journal of the American Chemical Society* **105**, 2159–2164.

Nishizaka, T., Oiwa, K., Noji, H., Kimura, S., Muneyuki, E., Yoshida, M. & Kinosita, Jr., K. (2004). Chemomechanical coupling in F1-ATPase revealed by simultaneous observation of nucleotide kinetics and rotation. *Nature Structural & Molecular Biology* **11**, 142–148.

Noji, H., Yasuda, R., Yoshida, M., Kinosita, Jr., K. (1997). Direct observation of the rotation of F1-ATPase. *Nature* **386**, 299.

Noyes, R. M. (1961). Effects of diffusion rates on chemical kinetics. *Progr. React. Kinet.* **1**, 129–160.

Oster, G. & Wang, H. (2000). Reverse engineering a protein: the mechanochemistry of ATP synthase. *Biochim. Biophys. Acta.* **1458**, 482–510.

Panke, O., Cherepanov, D. A., Gumbiowski, K., Engelbrecht, S. & Junge, W. (2001). Viscoelastic dynamics of actin filaments coupled to rotary F-ATPase: angular torque profile of the enzyme. *Biophysical Journal* **81**, 120–1233.

Pedersen, P. L. & Carafoli, E. (1987). Ion motive ATPases. I. Ubiquity, properties, and significance to cell function. *Trends in Biochemical Sciences* **4**, 146–150.

Sakaki, N., Shimo-Kon, R., Adachi, K., Itoh, H., Furuike, S., Muneyuki, E., Yoshida, M. & Kinosita, Jr., K. (2005). One rotary mechanism for F1-ATPase over ATP concentrations from millimolar down to nanomolar. *Biophysical Journal* **88**, 2047–2056.

Senior, A. E. (2007). ATP synthase: motoring to the finish line. *Cell* **130**, 220–221.

Sielaff, H., Martin, J., Singh, D., Biukovic, G., Gruber, G. & Frasch, W. D. (2016). Power stroke angular velocity profiles of archaeal A-ATP synthase *versus* thermophilic and mesophilic F-ATP synthase molecular motors. *Journal of Biological Chemistry* **291**, 25351–25363.

Sielaff, H., Rennekamp, H., Engelbrecht, S. & Junge, W. (2008). Functional halt positions of rotary F_OF_1-ATPase correlated with crystal structures. *Biophysical Journal* **95**, 4979–4987.

Spetzler, D., Ishmukhametov, R., Hornung, T., Day, L. J., Martin, J. & Frasch, W. D. (2009). Single molecule measurements of F1-ATPase reveal an interdependence between the power stroke and the dwell duration. *Biochem.* **48**, 7979.

Sugawa, M., Okazaki, K.-I., Kobayashi, M., Matsui, T., Hummer, G., Masaike, T. & Nishizaka, T. (2016). F1-ATPase conformational cycle from simultaneous single-molecule FRET and rotation measurements. *Proceedings of the National Academy of Sciences USA* **113**, E2916–E2924.

Sutin, N. (1966). The kinetics of organic reactions in solution. *Annual Review of Physical Chemistry* **17**, 119–172.

Uchihashi, T., Iino, R., Ando, T. & Noji, H. (2011). High-speed atomic force microscopy reveals rotary catalysis of rotorless F1-ATPase. *Science* **333**, 755–758.

Volkán-Kacsó, S. & Marcus, R. A. (2015). Theory for rates, equilibrium constants, and brønsted slopes in F1-ATPase single molecule imaging experiments. *Proc. Natl. Acad. Sci. USA* **112**, 14230–14235.

Volkán-Kacsó, S. & Marcus, R. A. (2016). Theory of controlled rotation experiments, predictions, tests and comparison with stalling experiments in F1-ATPase. *Proc. Natl. Acad. Sci. USA* **113**, 12029–12034.

Volkán-Kacsó, S. & Marcus, R. A. (2017a). Long binding events in single molecule controlled rotation in F1-ATPase: theory and experiment. *Proceedings of the National Academy of Sciences USA* **114**, 7272–7277.

Volkán-Kacsó, S. & Marcus, R. A. (2017b). Free, Stalled, and Controlled Rotation Single Molecule Experiments on F1-ATPase and Their Relationships (Chapter 2). In Photosynthesis and bioenergetics. (ed. J. Barber and A. V. RUBAN). Singapore: World Scientific Co., 35–53.

Walker, J. E. (2003). Nobel lectures, chemistry 1996–2000. In *ATP Synthesis by Rotary Catalysis* (ed. I. Grenthe). Singapore: World Scientific Publishing Co., 146–168.

Walker, J. E. (2013). The ATP synthase: the understood, the uncertain and the unknown. *Biochemical Society Transactions* **41**, 1–16.

Watanabe, R., Iino, R. & Noji, H. (2010). Phosphate release in F1-ATPase catalytic cycle follows ADP release. *Nature Chemical Biology* **6**, 814–820.

Watanabe, R. & Noji, H. (2014). Timing of inorganic phosphate release modulates the catalytic activity of ATP-driven rotary motor protein. *Nature Communications* **5**, 3486.

Watanabe, R., Okuno, D., Sakakihara, S., Shimabukuro, K., Iino, R., Yoshida, M. & Noji, H. (2012). Mechanical modulation of catalytic power on F1-ATPase. *Nature Chemical Biology* **8**, 86.

Weber, J. (2010). Structural biology: toward the ATP synthase mechanism. *Nature Chemical Biology* **6**, 794–795.

Weber, J. & Senior, A. E. (1997). Catalytic mechanism of F1-ATPase. *Biochimica et Biophysica Acta* **1319**, 19–58.

Yasuda, R., Noji, H., Yoshida, M., Kinosita, Jr., K. & Itoh, H. (2001). Resolution of distinct rotational substeps by submillisecond kinetic analysis of F1-ATPase. *Nature* **410**, 898–904.

Zimmermann, B., Diez, M., Zarrabi, N., Gräber, P. & Börsch, M. (2005). Movements of the ε-subunit during catalysis and activation in single membrane-bound H^+-ATP synthase. *EMBO* **24**, 2053–20063.

https://doi.org/10.1017/S0033583517000129 Published online by Cambridge University Press